

Pressure Stimulated Currents (PSC) in marble samples

Cimon Anastasiadis ⁽¹⁾, Dimos Triantis ⁽¹⁾, Ilias Stavrakas ⁽¹⁾ and Filippos Vallianatos ⁽²⁾

⁽¹⁾ Department of Electronics, Technological Educational Institution of Athens, Greece

⁽²⁾ Department of Natural Resources Engineering, Technological Institute of Crete, Greece

Abstract

The electrical behaviour of marble samples from Penteli Mountain was studied while they were subjected to uniaxial stress. The application of consecutive impulsive variations of uniaxial stress to thirty conatural samples produced Pressure Stimulated Currents (PSC). The linear relationship between the recorded PSC and the applied variation rate was investigated. The main results are the following: as far as the samples were under pressure corresponding to their elastic region, the maximum PSC value obeyed a linear law with respect to pressure variation. In the plastic region deviations were observed which were due to variations of Young's modulus. Furthermore, a special burst form of PSC recordings during failure is presented. The latter is emitted when irregular longitudinal splitting is observed during failure.

Key words Pressure Stimulated Currents (PSC)-Piezo Stimulated Current – rocks – marble-electric precursors

1. Introduction

Transient electric phenomena in the lithosphere have been observed for a long time (Varotsos and Alexopoulos, 1984a,b; Fujinawa and Takahashi, 1990; Nomicos and Vallianatos, 1997; Hayakawa, 1999). During the last decade, interest in transient electric signals has been growing and observation networks have been extended in many countries of the world (see Park *et al.*, 1993; Hayakawa, 1999; Kopytenko *et al.*, 2001; Hayakawa and Molchanov, 2002). Many models have been suggested to explain

such transient electric phenomena accompanied by fracture. Piezoelectric effects constitute one of several factors for modeling (*e.g.*, Finkelstein *et al.*, 1973). However the proposed mechanism cannot explain why non-piezoelectric minerals or rocks generate electric phenomena.

Moreover, electrokinetic effects (Mizutani *et al.*, 1976) are also limited to the cases of water-saturated rocks or water flowing through rocks. Since electric phenomena are also observed during fracturing of dried rocks it is evident that both piezoelectric and electrokinetic effects may not be the main factors for modeling such phenomena.

Many researchers accept that the transient electric phenomena are related to crack generation and propagation in the Earth's crust (*e.g.*, Molchanov and Hayakawa, 1995, 1998; Vallianatos and Tzanis, 1998, 1999a,b; Tzanis and Vallianatos, 2002).

In order to understand the mechanisms that produce these electric signals, many fracture tests in the laboratory have been conducted using various kinds of minerals and rocks under

Mailing address: Dr. Cimon Anastasiadis, Department of Electronics, Technological Educational Institution of Athens, Athens-Egaleo 12210, Greece; e-mail: cimon@teiath.gr

both dry and saturated conditions (*e.g.*, Nitsan, 1977; Ogawa *et al.*, 1985; Brady and Rowell, 1986; Cress *et al.*, 1987; Yamada *et al.*, 1989; Enomoto and Hashimoto, 1990; Hadjicontis and Mavromatou, 1994,1995; O’Keefe and Thiel, 1995; Freund, 2000; Takeuchi and Naghama, 2001; Stavrakas *et al.*, 2003).

Since transient electric phenomena are promising candidates as earthquake precursors, a series of laboratory experiments of uniaxial compression of marble samples were carried out to understand the underlying physical mechanisms of electric signal generation. In the first set of experiments, marble samples were subjected to a time-varying uniaxial compressional stress at both variable and constant stress rates, not exceeding the elasticity limit (Stavrakas *et al.*, 2003; Vallianatos *et al.*, 2004). The applied stress henceforth in the experiments is uniaxial compressional stress. The technique used to measure the current emitted from rock samples while applying stress at various rates will henceforth be referred to as pressure stimulated current technique. The experimental results support the validity of the Moving Charged Dislocation (MCD) model (see Vallianatos and Tzani 1998, 1999a,b; Tzani and Vallianatos, 2002).

In the present paper, we show experimental results obtained in the case of applying stress that produced deformations in the plastic range up to fracture. The results suggest that the proportionality factor γ between the emitted current (I) and the stress rate (dS/dt) changes as we pass to the plastic region, in consistency with the MCD model.

Furthermore, an experimental attempt to understand an electrical activity (*i.e.* a series of short pulses) observed approaching failure is given.

2. Sample and experimental description

Marble belongs to the class of metamorphic rocks. Its structural inhomogeneities are due to either natural or man-made causes such as the application of mechanical stress or chemical processing.

In the described experiment, thirty Dionysos marbles (see table I) collected from Mt. Penteli, Attica were used. The Dionysos marble, which has been typically used since ancient times for the construction of artifacts and monuments, is mainly composed of calcite (98%) and other minerals, depending on the variety of marble, such as muscovite, sericite and chlorite (Kleftakis *et al.*, 2000). Its content in quartz is very low, about 0.2%. Its density is 2.7 g/cm³ and its porosity is approximately 0.4%. Calcite crystals are polygonic, mainly equisized, sometimes exhibiting twinning and their texture may be characterized as *quasi*-homoblastic. The rock is white with a few thin parallel ash-green coloured veins containing silver-shaded areas due to the existence of chlorite and muscovite. Matrix rocks were intentionally selected to be *quasi* single-grained. The experiment was conducted in a Faraday shield to prevent electric noise. The noise-protected system comprised a uniaxial hydraulic load machine (Enerpac-RC106) that applied compressional stress to the sample, which was placed on a stainless steel base. The marble sample was placed between two thin teflon plates in the direction of stress to provide electrical insulation. The values of the externally applied stress were recorded using a manometer. A pair of electrodes was attached to the marble sample using conductive paste. The electrodes were attached in a direc-

Table I. Information table containing the samples used during the described experiments.

Sample code	Dimensions (mm)	Experimental technique applied
Marble Dionysos		
MD001 to MD010	50 × 50 × 50	PSC technique applied on sequential stress variations
MD011 to MD030	50 × 50 × 45	PSC measurements closely to the failure with constant stress rate

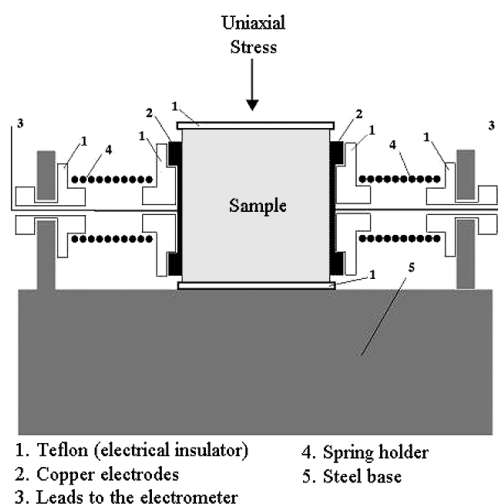


Fig. 1. Experimental setup.

tion perpendicular to the axis of the applied stress (see fig. 1). For electrical measurements, a sensitive programmable electrometer Keithley 617 was used, (current range from 0.1 fA to 20 mA).

3. Experimental results and discussion

In a set of previously conducted PSC experiments on marble samples (Stavarakas *et al.*, 2003; Vallianatos *et al.*, 2004), the samples were subjected to uniaxial stress in the elastic range of the material.

In the present set of experiments, multiple incremental stress variations were applied to the sample to pass progressively from the elastic into the plastic range.

Figure 2a-c shows the measured time series of the applied stress S (fig. 2a), the stress rate dS/dt (fig. 2b) and the current emission (fig. 2c) which is of the order of pA. The recording described corresponds to a stress range that the material behaves elastically. Our experimental data obey a scaling law relating the emitted current I and the stress rate dS/dt , (see Hadjiconitis and Mavromatou, 1994; Vallianatos and Tzannis, 1998, 1999a; Stavarakas *et al.*, 2003).

Recordings of the currents emitted due to successive abrupt changes of the applied stress both in regions where the material behaves elastically and in regions where the material is in the plastic range are shown in fig. 3a-c. Figure 3a depicts the sequence of steps of incremental stress variations. We note that the secondary axis was graded in values of normalized stress S/S_{\max} where S_{\max} is the maximum applied stress on the material close to failure. Figure 3b shows the stress rate dS/dt with respect to time. Figure 3c is the emitted current (I) with respect to time. We proceed now to the study of the relation between the emitted current (I) and the stress rate dS/dt , when the applied stress S takes values in both the elastic and plastic ranges. In

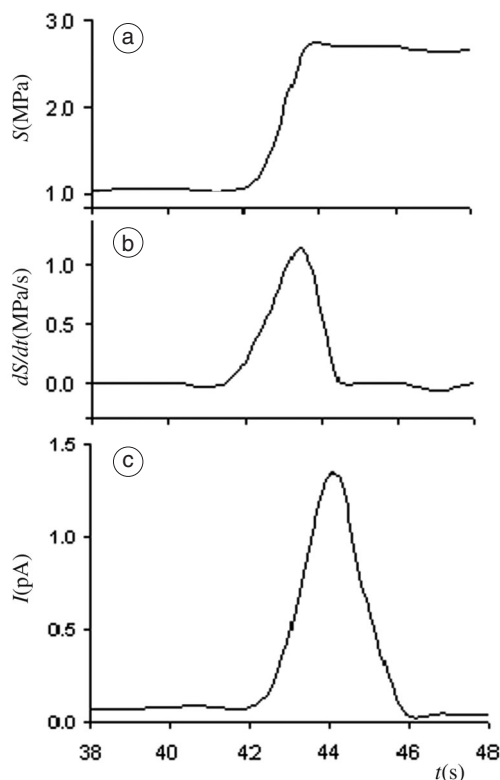


Fig. 2a-c. Time records of (a) stepwise applied stress to Penteli marble sample (MD007), b) the corresponding stress rate (ds/dt) and (c) the emitted PSC.

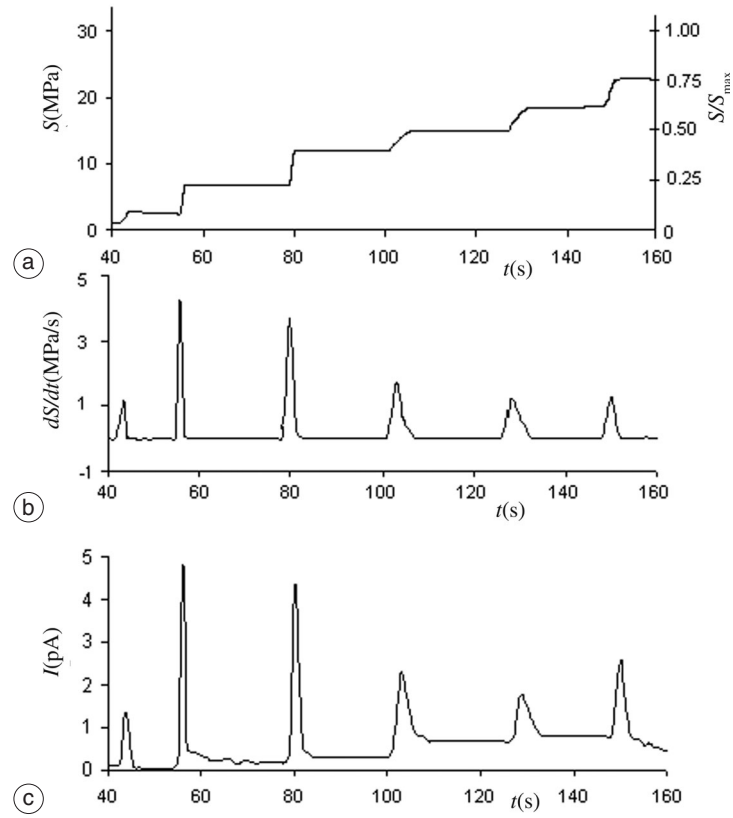


Fig. 3a-c. Time recordings of (a) successive abruptly applied stresses onto the sample (MD007), b) the corresponding stress rates and (c) PSC.

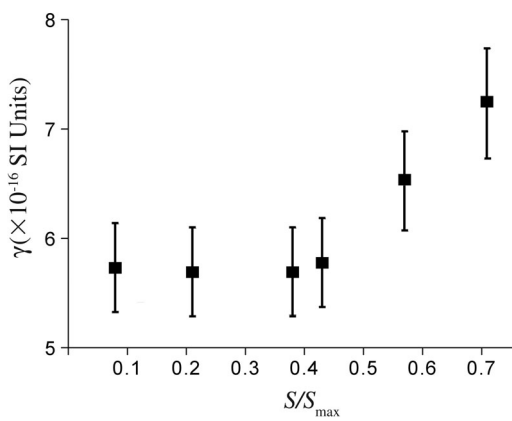


Fig. 4. Scaling factor γ with respect to the normalized stress.

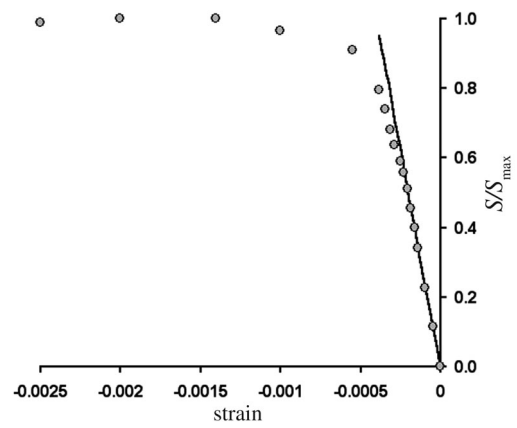


Fig. 5. Normalized experimental stress-strain diagram from a Penteli marble sample.

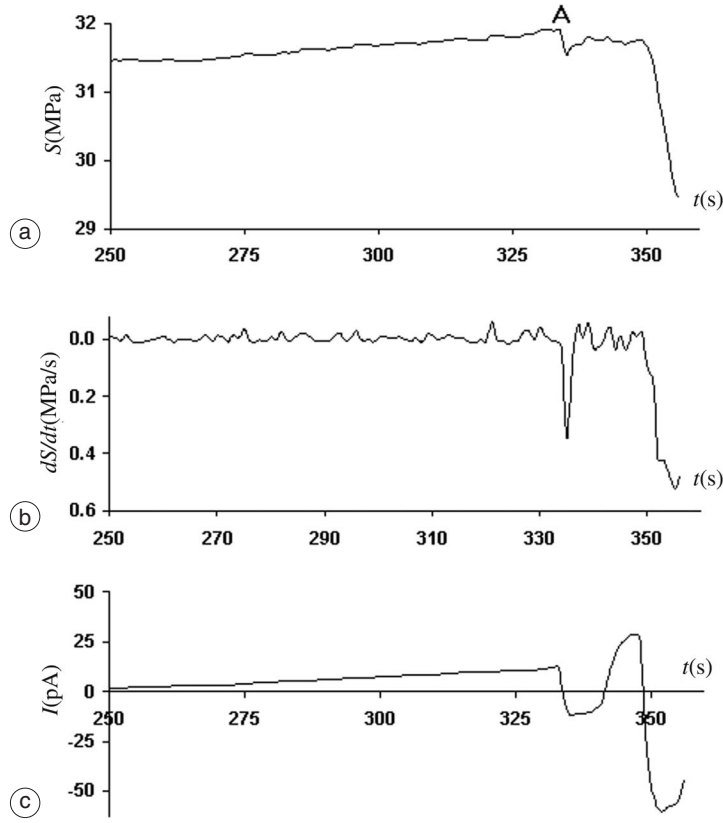


Fig. 6a-c. Time records of two PSC peaks taken from a marble sample (MD014) at fracture: a) curves, b) depict stress and (c) stress rate respectively.

previous papers, based on the MCD model, Valianatos and Tzanis (1998, 1999a) propose a scaling between the emitted current and the stress rate dS/dt , when the material is uniaxially compressed

$$I = \gamma \frac{dS}{dt} \quad (3.1)$$

where γ is a scaling factor which has a reciprocal dependence to the Young's modulus Y (i.e. $\gamma \sim 1/Y$) of the material.

Since we study the behaviour of marble samples in both the elastic and plastic ranges we may estimate the dependence of the scaling

factor γ on stress. Figure 4 demonstrates the dependence of factor γ on the normalized stress (S/S_{\max}). The scaling factor γ was calculated using the experimental data according to the relationship

$$\gamma = \frac{I_{\max}}{\left(\frac{dS}{dt}\right)_{\max}}$$

where I_{\max} is the maximum value of the emitted current during the application of uniaxial stress (S) and $(dS/dt)_{\max}$ is the corresponding maximum stress rate. In the calculation of the quantity S/S_{\max} , the stress S corresponds to its aver-

age value during each stress step. This is practically equal to the instantaneous stress on the sample at the time when the maximum value of the stress rate $(dS/dt)_{\max}$ is exerted. It becomes clear in the diagram of fig. 4 that when the applied stress is less than $0.5 S_{\max}$, the value of the factor γ remains practically constant. Noticeable is the fact that as far as $S/S_{\max} < 0.5$ the material behaves elastically and Young's modulus remains constant. This becomes evident in the normalized stress-strain diagram (fig. 5). The diagram was constructed using data of marble samples from Mt. Penteli, Attica (Kleftakis *et al.*, 2000). When the ratio $S/S_{\max} > 0.5$ the material exits the elastic range and gradually enters the plastic range thus Young's modulus Y is continuously decreasing.

According to the MCD model, the scaling factor γ is proportional to $1/Y$. This is consistent with the experimental result indicating that as the values of normalized stress S/S_{\max} increase, the factor γ increases too. The latter becomes evident if the calculated values of γ that correspond to the plastic range for $0.6 < S/S_{\max} < 0.7$ are considered (fig. 4). From the microphysical point of view we note that applying stresses in the plastic range, structural changes are introduced into the samples depending on the stress state. According to Hallbauer *et al.* (1973), when the sample is stressed uniaxially with stress beyond $0.55 S_{\max}$ up to $0.65 S_{\max}$ then microcracks appear. These cracks are the most dominant factor of all heterogeneities that govern the failure nucleation process in rock samples (Lei *et al.*, 2000) and are the sources of macrocracks that will appear when stress exceeds $0.85 S_{\max}$ and increases up to failure.

We proceed now to study PSC near the failure range. Figure 6a-c shows PSC emission when the applied stress was greater than $0.95 S_{\max}$. The continuously increasing stress on the sample and the corresponding stress rate dS/dt are depicted in fig. 6a and 6b respectively. The maximum recorded stress S_{\max} on the sample is recorded at $t = 334$ s, accompanied by a short abrupt decrease of the stress value. Simultaneously, the first current peak is recorded (fig. 6c). At the time interval between 340 s and 350 s stress was kept approximately constant and was followed by sample fracture accompanied by a

second more intense current peak. A photograph of the status of the specimen after the experiment is shown in fig. 7. The two main fracture planes (which were created while stress was instantaneously decreased) can be seen to lie along the direction of stress (point A in fig. 6a). Such fractures could be the result of a large number of microcracks that had already been generated when the sample had suffered a stress between $0.55 S_{\max}$ and $0.85 S_{\max}$ (Jaeger and Cook, 1979).

Systematic laboratory study of the PSC emitted by marble samples due to stress slightly before fracture suggests that when irregular longitudinal splitting is observed during the failure process (fig. 8a), then for each fracture plane corresponding to a macrocrack a PSC peak is observed. Thus, the number of PSC peaks appearing just before dynamic failure is



Fig. 7. Sample photo after fracture to show the fracture planes (sample: MD027).

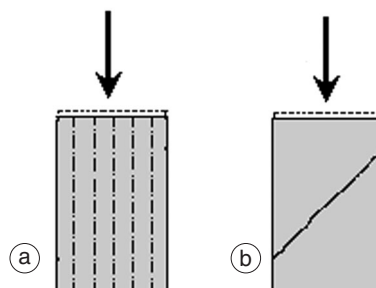


Fig 8a,b. Fracture modes of geomaterials: a) planes parallel to the direction of stress, b) planes diagonal to the direction of stress.

associated with the number of macrocracks created in directions nearly parallel to the direction of the applied stress. The experimental stressing of marble samples with multiple failure planes (*i.e.* similar to the one depicted in

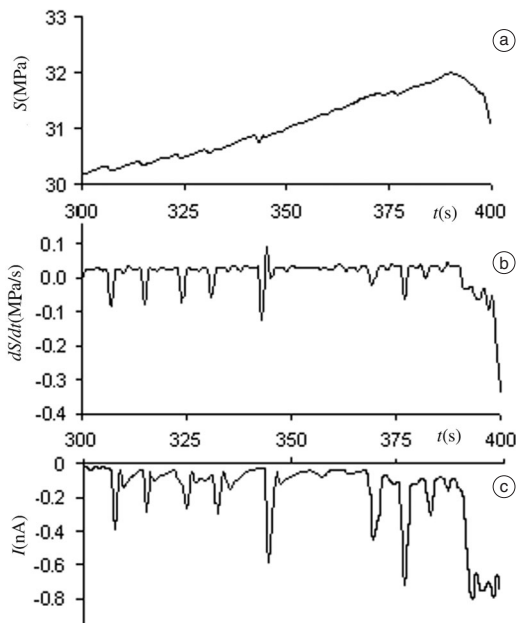


Fig. 9a-c. Multiple PSC peaks of a marble sample (MD016) in the time interval of the appearance of microcracks (parallel to the direction of the applied stress) and fracture time: a) stress, b) stress rate and (c) PSC.

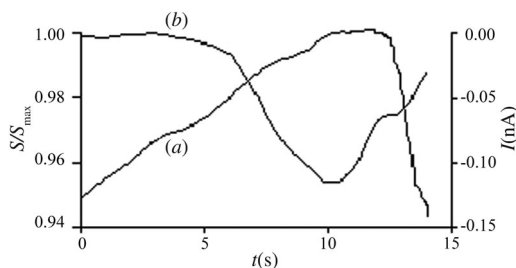


Fig. 10. PSC peak at diagonal fracture of a marble sample (MD018). Curve (a) corresponds to stress changes on a normalized axis; curve (b) corresponds to PSC.

fig. 7) gave multiple PSC peaks (see fig. 9a-c). On the other hand, when the failure of the sample forms a shear fracture, then a «single» PSC peak is observed (see fig. 10). The latter experimental results could possibly be related to the two types of electric earthquake precursors (*i.e.* single signals and electrical activities) reported by Varotsos and Lazaridou (1991).

4. Concluding remarks

In this paper, Pressure Stimulated Currents (PSC) were studied on a typical geomaterial (Penteli marble).

We first established a correlation between the emitted PSC and the applied stress rate. When the material was stressed within its elastic range, a linear relation between PSC and stress rate (dS/dt) was observed. Deviation from linearity exists when the applied stress on the geomaterial is driven to the plastic range. This is due to the dependence of the scaling factor between PSC and stress rate on Young's modulus.

We have shown that slightly before fracture, PSC emissions were detected associated with the fracture mode of the geomaterial. When the failure of the sample forms a shear fracture, then a «single» PSC peak is detected. When irregular longitudinal splitting is observed during the failure process then a PSC sequence is recorded which may suggest that each fracture plane corresponding to a macrocrack activates an electrical process.

REFERENCES

- BRADY, B.T. and G.A. ROWELL (1986): Laboratory investigation of the electrodynamics of rock fracture, *Nature*, **321**, 488-492.
- CRESS, G.O., B.T. BRADY and G.A. ROWELL (1987): Sources of electromagnetic radiation from fracture of rock samples in laboratory, *Geophys. Res. Lett.*, **14**, 331-334.
- ENOMOTO, J. and H. HASHIMOTO (1990): Emission of charged particles from indentation fracture of rocks, *Nature*, **346**, 641-643.
- FINKELSTEIN, D., R.D. HILL and J.R. POWELL (1973): The piezoelectric theory of earthquake lightning, *J. Geophys. Res.*, **78**, 992-993.
- FREUND, F. (2000): Time-resolved study of charge genera-

- tion and propagation in igneous rocks, *J. Geophys. Res.*, **105** (B5), 11001-11019.
- FUJINAWA, Y. and K. TAKAHASHI (1990): Emission of electromagnetic radiation preceding the Ito seismic swarm of 1989, *Nature*, **347**, 376-378.
- HADJICONTIS, V. and C. MAVROMATOU (1994): Transient electric signals prior to rock failure under uniaxial compression, *Geophys. Res. Lett.*, **21**, 1687-1690.
- HADJICONTIS, V. and C. MAVROMATOU (1995): Electric signals recorded during uniaxial compression of rock samples: Their possible correlation with preseismic electric signals, *Acta Geophys. Polon.*, **43**, 49-61.
- HALLBAUER, D.K. H. WAGNER and N.G.W. COOK (1973): Some observations concerning the microscopic and mechanical behaviour of quartzite specimens in stiff, triaxial compression tests, *Int. J. Rock Mech. Min Sci. Geomech. Abstr.*, **10**, 713-726.
- HAYAKAWA, M. (Editor) (1999): *Atmospheric and Ionospheric Electromagnetic Phenomena Associated with Earthquakes* (Terra Scientific Publishing Co., Tokyo), pp. 996.
- HAYAKAWA, M. and O. MOLCHANOV (Editors) (2002): *Seismo Electromagnetics: Lithosphere-Atmosphere-Ionosphere Coupling* (Terra Scientific Publishing Co., Tokyo), pp. 477.
- JAEGER, J.C. and N.G.W. COOK (1979): *Fundamentals of Rock Mechanics* (Chapman and Hall, London), pp. 593.
- KLEFTAKIS, S., Z. AGIOUTANTIS and C. STIAKAKIS (2000): Numerical simulation of the uniaxial compression test including the specimen-platen interaction, in *Computational Methods for Shell and Spatial Structures* (IASS-IACM).
- KOPYTENKO, Y., V. ISMAGILOV, M. HAYAKAWA, N. SMIRNOVA, V. TROYAN and T. PETERSON (2001): Investigation of the ULF electromagnetic phenomena related to earthquakes: contemporary achievements and perspectives, *Ann. Geofis.*, **44** (2), 325-334.
- LEI, X.L., K. KUSUNOSE, O. NISHIZAWA, A. CHO and T. SATOH (2000): On the spatiotemporal distribution of acoustic emissions in two granitic rocks under triaxial compression: the role of pre-existing cracks, *Geophys. Res. Lett.*, **27**, 1997-2000.
- MIZUTANI, H., T. ISHIDO, T. YOKOKURA and S. OHNISHI (1976): Electrokinetic phenomena associated with earthquakes, *Geophys. Res. Lett.*, **3**, 365-368.
- MOLCHANOV, O.A. and M. HAYAKAWA (1995): Generation of ULF electromagnetic emissions by microfracturing, *Geophys. Res. Lett.*, **22**, 3091-3094.
- MOLCHANOV, O.V. and M. HAYAKAWA (1998): On the generation mechanism of ULF seismogenic electromagnetic emissions, *Physic. Earth Planet. Int.*, **105**, 201-210.
- NITSAN, U. (1977): Electromagnetic emission accompanying fracture of quartz-bearing rocks, *Geophys. Res. Lett.*, **4**, 333-337.
- NOMICOS, K. and F. VALLIANATOS (1997): Transient electric variations associated with large intermediate-depth earthquakes in South Aegean, *Tectonophysics*, **269**, 171-177.
- OGAWA, T., K. OIKE and T. MIURA (1985): Electromagnetic radiation from rocks, *J. Geophys. Res.*, **90**, 6245-6249.
- O'KEEFE, S.G. and D.V. THIEL (1995): A mechanism for the production of electromagnetic radiation during fracture of brittle materials, *Physic. Earth Plane. Inter.*, **89**, 127-135.
- PARK, S.K., M.J.S. JOHNSTON, T.R. MADDEN, F.D. MORGAN and H.F. MORRISON (1993): Electromagnetic precursors to earthquakes in the ULF band: a review of observations and mechanisms, *Rev. Geophys.*, **31**, 117-132.
- STAVRAKAS, I., C. ANASTASIADIS, D. TRIANTIS and F. VALLIANATOS (2003): Piezo stimulated currents in marble samples: Precursory and concurrent-with-failure signals, *Nat. Hazards Earth Syst. Sci.*, **3**, 243-247.
- TAKEUCHI, A. and H. NAGAHAMA (2001): Voltage changes induced by stick-slip of granites, *Geophys. Res. Lett.*, **28**, 3365-3367.
- TZANIS, A. and F. VALLIANATOS (2002): A physical model of electrical earthquake precursors due to crack propagation and the motion of charged edge dislocations, in *Seismo Electromagnetics: Lithosphere-Atmosphere-Ionosphere Coupling*, edited by M. HAYAKAWA and O.A. MOLCHANOV (Terra Scientific Publishing Co., Tokyo), 117-130.
- VALLIANATOS, F. and A. TZANIS (1998): Electric current generation associated with the deformation rate of a solid: preseismic and coseismic signals, *Phys. Chem. Earth*, **23**, 933-938.
- VALLIANATOS, F. and A. TZANIS (1999a): A model for the generation of precursory electric and magnetic fields associated with the deformation rate of the earthquake focus, in *Atmospheric and Ionospheric Electromagnetic Phenomena Associated with Earthquakes*, edited by M. HAYAKAWA (Terra Scientific Publishing Co., Tokyo), 287-305.
- VALLIANATOS, F. and A. TZANIS (1999b): On possible scaling laws between Electric Earthquake Precursors (EEP) and earthquake magnitude, *Geophys. Res. Lett.*, **26** (13), 2013-2016.
- VALLIANATOS, F., D. TRIANTIS, A. TZANIS, C. ANASTASIADIS and I. STAVRAKAS (2004): Electric earthquake precursors: from laboratory results to field observations, *Phys. Chem. Earth*, **29**, 339-351.
- VAROTSOS, P. and K. ALEXOPOULOS (1984a): Physical properties of the variations of the electric field of the Earth preceding earthquakes, 1, *Tectonophysics*, **110**, 73-98.
- VAROTSOS, P. and K. ALEXOPOULOS (1984b): Physical properties of the variations of the electric field of the Earth preceding earthquakes, 2. Detection of epicentre and magnitude, *Tectonophysics*, **110**, 99-125.
- VAROTSOS, P. and M. LAZARIDOU (1991): Latest aspects of earthquake prediction in Greece based on seismic electric signals, *Tectonophysics*, **188**, 321-347.
- YAMADA, I., K. MASUDA and H. MIZUTANI (1989): Electromagnetic and acoustic emission associated with rock fracture, *Phys. Earth Planet. Inter.*, **57**, 157-168.